A New Scale Space Total Variation Algorithm for Limited Angle Tomography

Yixing Huang*, Oliver Taubmann*‡, Xiaolin Huang*, Viktor Haase§, Guenter Lauritsch† and Andreas Maier*‡
*Pattern Recognition Lab, Friedrich-Alexander-University Erlangen-Nuremberg, Erlangen, Germany
†Siemens Healthcare GmbH, Forchheim, Germany
‡Erlangen Graduate School in Advanced Optical Technologies (SAOT), Erlangen, Germany
§Institute for Signal Processing, University of Luebeck, Luebeck, Germany

Email: yixing.yh.huang@fau.de

***Abstract*—This paper proposes a scale space total variation (ssTV) algorithm to reduce large scale streaks in limited angle tomography. The weighted total variation (wTV) algorithm is able to remove most small scale streaks. However, it fails to reduce larger streaks since total variation (TV) regularization is scale-dependent and may regard them as homogeneous areas. Derived from the wTV algorithm, the proposed ssTV algorithm applies wTV regularization on the image at different scales using down-sampling and up-sampling operations and thus can reduce streaks more effectively. Advantages of the ssTV algorithm are demonstrated on both 2-D numerical data and a 3-D clinical dataset.**

I. Introduction

Limited angle tomography is an essential but challenging task in practical applications of computed tomography (CT). The limited angle problem arises when the gantry rotation is restricted by other system parts or scanning time. Due to data incompleteness, the reconstructed images have severe streak artifacts and obtaining high quality images is difficult.

Researchers have put a lot of effort into suppressing streak artifacts in limited angle reconstruction. One approach is to recover the missing sinogram data in the projection domain based on data consistency conditions like Ludwig-Helgason consistency [1]. In addition, iterative reconstruction with total variation (TV) regularization algorithms [2]–[4] was demonstrated to be effective in limited angle tomography since compressed sensing technologies can use relatively few data to achieve good image quality with the prior assumption that medical images are sparse in the gradient domain.

In the case of limited angle tomography, the shape and orientation of streak artifacts are closely related to the angles missing in the acquisition. With this additional prior information, Chen et al. [5] developed the anisotropic TV (aTV) by assigning different weighting factors to different directions, which shows better performance on edge recovery and streak artifact reduction than the isotropic TV algorithm. However, some structures in the clinical reconstructed image may be blurred due to the staircasing effect [6].

The weighted TV (wTV) algorithm proposed by Candès et al. [7] can help avoid this effect. In our previous work [8], we demonstrated that wTV can reduce noise well while preserving image resolution and contrast in the case of complete data.

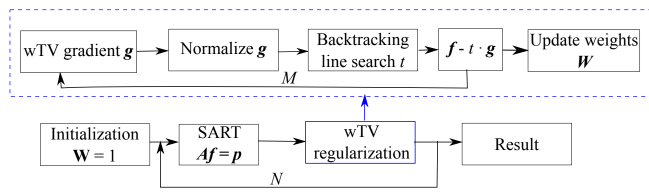

Fig. 1. The wTV algorithm iterates SART and wTV regularization steps alternatively N times in the outer loop. The wTV regularization step repeats the gradient descent process M times as the inner loop.

In the limited angle case, wTV can reduce small streaks well yet is unable to remove large streaks. Due to the scale-dependent property of TV regularization [9], large streaks may be regarded as homogeneous areas and real edges. To enhance homogeneity particularly along the streaks' normal direction, we proposed the weighted anisotropic TV (waTV) algorithm [8] by using four neighboring pixels instead of two to calculate the gradient along that direction. The waTV algorithm showed promising potential in streak reduction. However, it may produce new "zebra crossing"-like artifacts. Besides, it is cumbersome to incorporate anisotropy analytically since new formulas need to be derived for different scales. With the aims of enabling convenient implementation and avoiding zebra crossing artifacts while reducing streaks of various sizes, the scale space TV (ssTV) algorithm is proposed in this paper.

II. Methods

The reconstruction model of the wTV algorithm can be

$$\min_{\boldsymbol{f}} ||\boldsymbol{f}||_{\mathrm{wTV}} \quad \text{subject to} \quad \boldsymbol{Af} = \boldsymbol{p}, \tag{1}$$

where $\boldsymbol{f}$ is the image, $\boldsymbol{A}$ is the system matrix and $\boldsymbol{p}$ is the acquired projection data. Based on Candès et al. [7], $||\boldsymbol{f}||_{\mathrm{wTV}}$ is defined as

$$\begin{aligned} ||\boldsymbol{f}||_{\mathrm{wTV}} &= \sum_{x,y,z} \boldsymbol{W}_{x,y,z} || \left(\mathcal{D}\boldsymbol{f}\right)_{x,y,z} ||, \\ \boldsymbol{W}_{x,y,z} &= \frac{1}{||(\mathcal{D}\boldsymbol{f})_{x,y,z}|| + \epsilon}, \end{aligned} \tag{2}$$

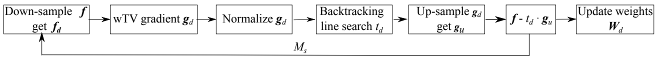

Fig. 2. The ssTV minimization substep down-samples the image $\boldsymbol{f}$ to calculate the down-sampled wTV gradient $\mathbf{g}_d$ and step size t_d, then it uses t_d and the up-sampled $\mathbf{g}_u$ to update the original image $\boldsymbol{f}$.

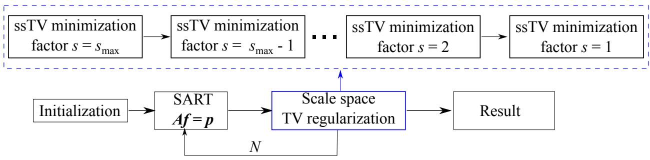

Fig. 3. The ssTV algorithm uses multiple scales during wTV regularization. See Fig. 2 for an overview of the ssTV minimization step.

where $\boldsymbol{W}$ is the weight matrix, $\mathcal{D}\boldsymbol{f}$ is the gradient of $\boldsymbol{f}$, x, y and z are pixel indices and ϵ is a parameter influencing the reconstructed image resolution. The flow chart of the whole algorithm is shown in Fig. 1. The main loop iterates at most N times and each iteration consists of a simultaneous algebraic reconstruction technique (SART) [10] step to increase data fidelity as well as a wTV regularization step. In each wTV regularization step, we regard the weight matrix $\boldsymbol{W}$ as constant for computing the gradient of $||\boldsymbol{f}||_{\text{wTV}}$ with respect to the image to retain a convex problem [7],

$$\boldsymbol{g}_{x,y,z} = \frac{\partial ||\boldsymbol{f}||_{\text{wTV}}}{\partial \boldsymbol{f}_{x,y,z}}, \tag{3}$$

and repeat the gradient descent process M times using backtracking line search algorithm [11]. After that, $\boldsymbol{W}$ is updated.

The effects of conventional TV regularization are often quite local [9]. It mostly reduces small streaks well while larger streaks remain essentially intact. We assume that if we apply TV regularization at various resolutions using a scale-space approach, larger streaks may also be reduced well. This is the main idea of our proposed ssTV algorithm.

Fig. 2 is an ssTV minimization substep. It first down-samples the image $\boldsymbol{f}$ with a certain scaling factor s to calculate the down-sampled wTV gradient $\mathbf{g}_d$ and find a suitable step size t_d to make sure that the TV value of $\boldsymbol{f}_d - t_d \cdot \mathbf{g}_d$ is decreased. With the down-sampling operation, the scale of the streaks is decreased relative to the spatial gradient computation used in TV. Then $\mathbf{g}_d$ is up-sampled with the same scaling factor s to get $\mathbf{g}_u$, which means that the scale of TV regularization effects are increased. Finally, with t_d and $\mathbf{g}_u$ the original scale image $\boldsymbol{f}$ can be updated as $\boldsymbol{f} - t_d \cdot \mathbf{g}_u$. The above process is repeated M_s times, then the corresponding weight matrix $\boldsymbol{W}_d$ is updated.

In limited angle tomography, orientations of streaks can be aligned with a coordinate axis, e.g. the X-axis, if we choose a proper corresponding scan angle range 10° - 170° (Fig. 4) such that anisotropic scaling along Y direction can be performed.

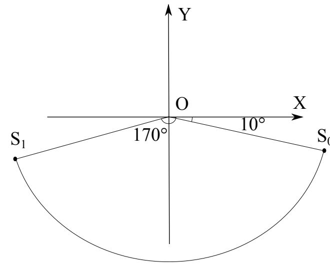

Fig. 4. Scan trajectory.

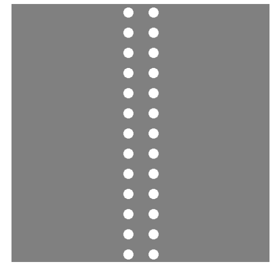

Fig. 5. Numerical phantom, window: [-240 240] HU.

The down-sampling and up-sampling operations with a scaling factor $s > 1$ are defined as

$$\begin{aligned}
\boldsymbol{f'}_{x,y,z} &= \sum_{j=-L}^{j=L} \boldsymbol{h}_{j+L} \boldsymbol{f}_{x,y+j,z}, \\
(\boldsymbol{f}_d)_{x,y,z} &= \left(\sum_{j=0}^{j=s-1} \boldsymbol{f'}_{x,s\cdot y+j,z} \right) / s, \\
\boldsymbol{f}_{x,s\cdot y+j,z} &= \Big((\boldsymbol{f}_d)_{x,y,z} \cdot (s-j) + (\boldsymbol{f}_d)_{x,y+1,z} \cdot j \Big) / s, \\
& \quad j = 0, 1, ..., s-1,
\end{aligned} \tag{4}$$

where $\boldsymbol{h}$ is a 1-D Gaussian filter kernel with length $2L+1$ and standard deviation $\sigma = s/2$ to avoid aliasing and $\boldsymbol{f'}$ is the filtered image.

As regularization on a single scale is most sensitive to artifacts of a specific spatial extent, we perform it in scale space, i.e. on several scales, $s = s_{\max}, s_{\max} - 1, ..., 2, 1$ with increasing resolution (Fig. 3), where $s_{\max}$ is the maximum scaling factor. In this way, both noise and streaks of various sizes can be reduced. Note that ssTV minimization with $s = 1$ is the regular wTV minimization.

III. EXPERIMENTS

A. Numerical Phantom

In order to validate the advantage of our proposed ssTV algorithm in reducing large streaks, a 2-D numerical phantom is designed (Fig. 5). It contains two columns of circular areas (radius = 10 mm). The attenuation coefficient for the circular areas is 1200 HU while the background is 0 HU. The phantom size is 512×512 pixels and the pixel size is 1 mm. Regarding the acquisition parameters, the scan angle from 10° to 170° is chosen such that most streaks are almost in the horizontal direction. The detector size is 768 pixels and the pixel size is 1 mm. The source to detector distance is $d = 2175$ mm, the fan angle is $\gamma_{\max} = 20°$ and the angular increment is 1°. The whole experimental setup, including generation of the phantoms, is implemented in CONRAD [12].

The ssTV algorithm and the regular wTV algorithm are employed to reconstruct this phantom from limited angle data. For wTV, we choose $M = 10$ heuristically. Consequently, for ssTV, the same number of TV minimization steps should be applied, i.e. $\sum_{s=1}^{\infty} M_s = M = 10$. With this constraint, combinations of different scaling factors are investigated as follows: $[M_1, M_2, M_3, M_4, M_5]$ = [2, 8, 0, 0, 0], [2, 4, 4, 0, 0], [2, 2, 2, 4, 0] and [2, 2, 2, 2, 2]. Besides, ssTV with $s = 2$ only, i.e. $[M_1, M_2, M_3, M_4, M_5]$ = [0, 10, 0, 0, 0], is also investigated as a control.

All images, including clinical data described below, are reconstructed with $\epsilon = 0.001$ in Eqn. 2. The reconstruction algorithms stop when they reach the termination criteria $\sigma < 8.0 \cdot 10^{-3}$ HU or $n = 400$, where σ is the root-mean-square difference of two consecutive iteration results and n is the iteration number.

B. Clinical Data

The algorithms are also compared in a 3-D clinical head dataset acquired with a Siemens Artis zee angiographic C-arm system (Siemens Healthcare GmbH, Forchheim, Germany). The detector size is 1240×960 and the detector pixel size is 0.308 mm. The complete data contains 496 projections obtained in a 200° short scan. We simulate a limited angle acquisition with a scan angle from 10° to 170° where only the projections 25 through 422 are used. The reconstruction image grid size is $512 \times 512 \times 256$, and the pixel sizes are 0.4 mm, 0.4 mm and 0.8 mm in X, Y and Z direction, respectively.

We first use the wTV algorithm to reconstruct the complete data as an image quality reference. Then, wTV and ssTV are applied to the limited angle data. In [8], we determined that it is beneficial to apply 30 iterations of SART first as initialization, then 50 additional iterations of wTV or ssTV are applied.

IV. Results And Discussion

The reconstruction results of the numerical phantom and their root-mean-square errors (RMSE) are shown in Fig. 6. Large streaks still exist in the wTV reconstruction result (Fig. 6(a)) while they are reduced by ssTV with $s = 2$ (Fig. 6(b)). However, ssTV with scaling factor 2 only is unable to reduce high frequency noise. In contrast, ssTV with $s_{\max} = 2$ (Fig. 6(c)) and $s_{\max} = 3$ (Fig. 6(d)) can reduce both large streaks and high frequency noise effectively. Fig. 7 also demonstrates that combinations of multiple scaling factors (curves C, D, E and F) converge faster than wTV (curve A) while using scale 2 only (curve B) is insufficient.

The reference images reconstructed from the complete clinical dataset with wTV are shown in Fig. 8. Image results of SART, wTV and ssTV for limited angle tomography are shown in Fig. 9. Compared to SART (Figs. 9(a) and 9(b)), wTV shows its advantage in reducing small streaks and high frequency noise since the bony structures and the brain textures are preserved much better. However, severe large streaks still remain in the wTV results (Figs. 9(c) and 9(d)). The proposed ssTV algorithm with $s = 2$ only can reduce large streaks better than wTV. However, Fig. 9(f) shows that it suffers from severe high frequency noise like the SART result and thus the brain texture is obscured. This confirms that combining various scaling factors is beneficial for reducing noise and streaks of various sizes. Figs. 9(g) - (j) illustrate that ssTV with $s_{\max} \geq 2$ can reduce large streaks more effectively while high frequency noise is also removed.

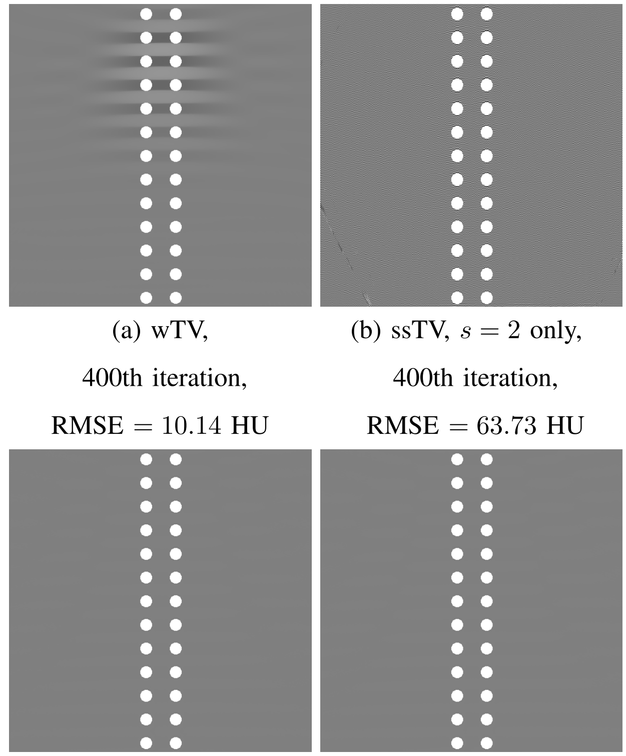

(a) wTV, 400th iteration, RMSE = 10.14 HU

(b) ssTV, $s = 2$ only, 400th iteration, RMSE = 63.73 HU

(c) ssTV, $s_{\max} = 2$, 341th (final) iteration, RMSE = 0.79 HU

(d) ssTV, $s_{\max} = 3$, 328th (final) iteration, RMSE = 0.55 HU

Fig. 6. Comparison of wTV, ssTV with $s = 2$ only, $s_{\max} = 2$ and $s_{\max} = 3$, windowing: [-240 240] HU, (a) $M = 10$, (b) $[M_1, M_2] = [0, 10]$, (c) $[M_1, M2] = [2, 8]$, (d) $[M_1, M_2, M_3] = [2, 4, 4]$.

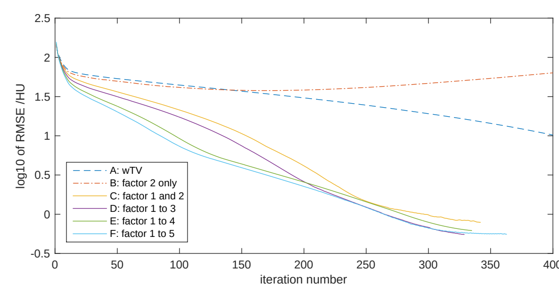

Fig. 7. Comparison of different scaling factor combinations, $M = 10$ for A, $[M_1, M_2, M_3, M_4, M_5]$ =[0, 10, 0, 0, 0], [2, 8, 0, 0, 0], [2, 4, 4, 0, 0], [2, 2, 2, 4, 0] and [2, 2, 2, 2, 2] for B, C, D, E and F, respectively.

V. Conclusion

In this paper, we proposed the ssTV algorithm for streak reduction in limited angle tomography. From the experiments above, we conclude that the ssTV algorithm with various scaling factors converges faster and reduces large streaks better than wTV. It is convenient to implement based on an existing

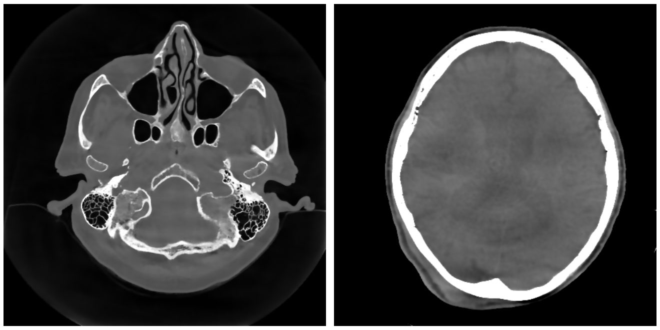

(a) wTV, 65th slice (b) wTV, 140th slice

Fig. 8. Reference images reconstructed from the complete clinical dataset with the wTV algorithm. Windowing: [-1000 1730] HU for (a) and [-220 365] HU for (b).

wTV implementation as it only introduces additional down-sampling and up-sampling operations.

Disclaimer: The concepts and information presented in this paper are based on research and are not commercially available.

REFERENCES

[1] J. L. Prince and A. S. Willsky, "Constrained sinogram restoration for limited-angle tomography," *Optical Engineering*, vol. 29, no. 5, pp. 535–544, 1990.

[2] M. T. Manhart, M. Kowarschik, A. Fieselmann, Y. Deuerling-Zheng, K. Royalty, A. K. Maier, and J. Hornegger, "Dynamic iterative reconstruction for interventional 4-D C-arm CT perfusion imaging," *Medical Imaging, IEEE Transactions on*, vol. 32, no. 7, pp. 1336–1348, 2013.

[3] H. Wu, A. Maier, R. Fahrig, and J. Hornegger, "Spatial-temporal total variation regularization (STTVR) for 4D-CT reconstruction," in *Proc of SPIE*, vol. 8313, 2012.

[4] E. Sidky, C. Kao, and X. Pan, "Accurate image reconstruction from few-views and limited-angle data in divergent-beam CT," *Journal of X-ray science and technology*, vol. 14, pp. 119–139, 2006.

[5] Z. Chen, X. Jin, L. Li, and G. Wang, "A limited-angle CT reconstruction method based on anisotropic TV minimization," *Physics in medicine and biology*, vol. 58, no. 7, pp. 2119–2141, 2013.

[6] V. Y. Panin, G. L. Zeng, and G. T. Gullberg, "Total variation regulated EM algorithm," *Nuclear Science, IEEE Transactions on*, vol. 46, pp. 2202 – 2210, 1999.

[7] E. Candès, M. Wakin, and S. Boyd, "Enhancing sparsity by reweighted l_1 minimization," *The journal of fourier analysis and applications*, vol. 14, pp. 877–905, 2008.

[8] Y. Huang, O. Taubmann, X. Huang, V. Haase, G. Lauritsch, and A. Maier, "A new weighted anisotropic total variation algorithm for limited angle tomography," in *International Symposium on Biomedical Imaging*. IEEE, 2016, to appear.

[9] D. Strong and T. Chan, "Edge-preserving and scale-dependent properties of total variation regularization," *Inverse Problems*, vol. 19, no. 6, p. S165, 2003.

[10] L. Ritschl, F. Bergner, C. Fleischmann, and M. Kachelriess, "Improved total variation-based CT image reconstruction applied to clinical data," *Physics in medicine and biology*, vol. 56, no. 6, pp. 1545–1561, 2011.

[11] S. Boyd and L. Vandenberghe, *Convex Optimization*. Cambridge University Press, 2004.

[12] A. Maier, H. Hofmann, M. Berger, P. Fischer, C. Schwemmer, H. Wu, K. Müller, J. Hornegger, J. Choi, C. Riess, A. Keil, and R. Fahrig, "CONRAD - a software framework for cone-beam imaging in radiology," *Medical physics*, vol. 40, no. 11, p. 111914, 2013.

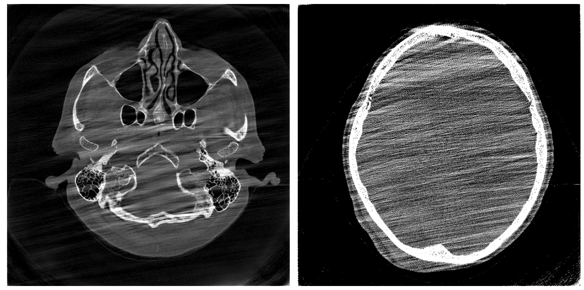

(a) SART as initialization (b) SART as initialization

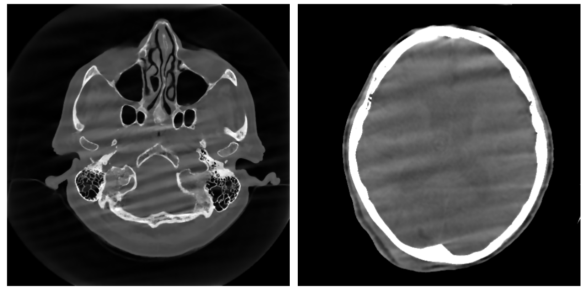

(c) wTV (d) wTV

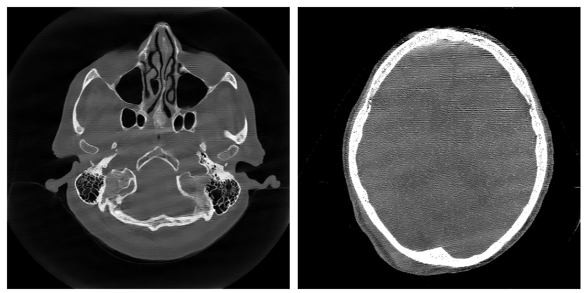

(e) ssTV, $s = 2$ only (f) ssTV, $s = 2$ only

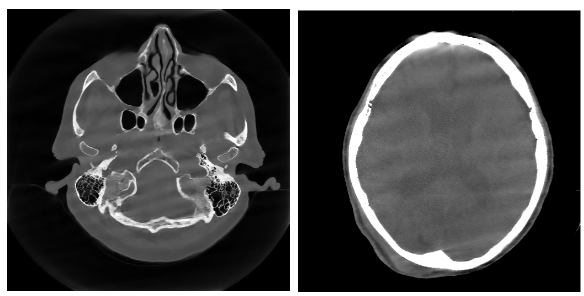

(g) ssTV, $s_{\max} = 2$ (h) ssTV, $s_{\max} = 2$

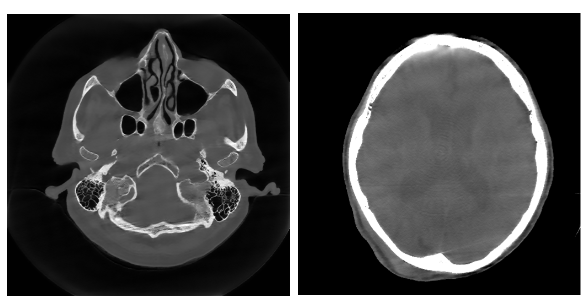

(i) ssTV, $s_{\max} = 3$ (j) ssTV, $s_{\max} = 3$

Fig. 9. Comparison of SART, wTV, ssTV with $s = 2$ only and $s_{\max} = 2, 3$ in limited angle tomography, $M = 10$ for wTV, $[M_1, M_2, M3] = [0, 10, 0]$, $[2, 8, 0]$ and $[2, 4, 4]$ for ssTV with $s = 2$ only, $s_{\max} = 2$ and $s_{\max} = 3$, respectively. Windowing: [-1000 1730] HU for the left images, [-220 365] HU for the right images.